

HEAT TRANSFER INVESTIGATION OF THE SUB- AND SUPERCRITICAL FUEL FLOW THROUGH A U-TURN TUBE

Zhang C B*, Tao Z, Xu G Q, Deng H W, Sun J N
National Key Lab. on Aero-Engines, School of Jet Propulsion,
BUAA, Beijing, 100191, China
(* Corresponding author: zhang_cb@sjp.buaa.edu.cn)

ABSTRACT. This paper was to experimentally study the heat transfer characteristics within an air/fuel heat exchanger in an attempt to cool the cooling air from the compressor with RP3 kerosene as the coolant and at the same time heat it up over its critical temperature. The supercritical fuel was then injected into the combustor while the cooled cooling air was led to the turbine for blade and disk cooling.

In the experiments, a series of U-turn tubes were heated from outside and the RP-3 flowed through them at supercritical pressures ($p_{red} \sim 2$). The test section inlet Reynolds number and the bend diameter (BD/d) of the U-turn tube were the two main influencing factors under consideration and the outside wall heat flux was varied to keep the exit fuel temperatures over its critical temperature. Test results indicated that the heat transfer coefficients were monotonously increasing along the tube for all experimental runs. In the bend regions, the heat transfer was enhanced due to the strong secondary flow induced by the centrifugal force and however, the enhancement was not obvious for low Reynolds number cases.

EXPERIMENTAL APPARATUS AND PROCEDURES

Facility A simplified schematic of the experimental system is shown in Fig. 1, the test section

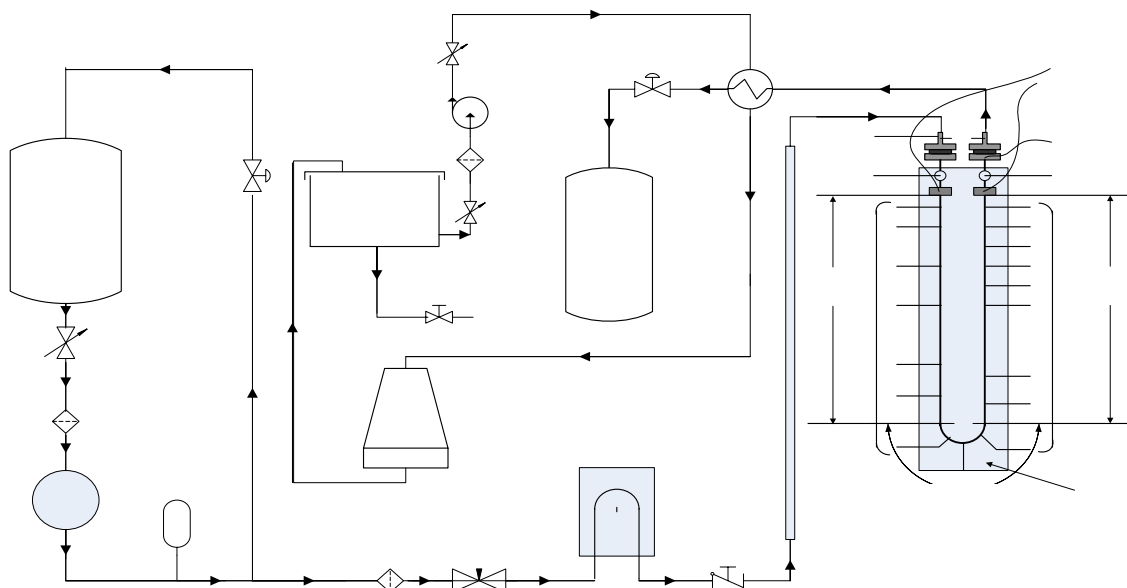


Figure 1. Schematic of the supercritical fluid system

was mounted vertically and isolated with Aspen, and it was heated up by passing a current through the tube and the amount of energy input was determined by recording the voltage and current applied. Four alternating current power supplies were available and each capable of 20kW. The heat losses to the environment via the isolation was verified to be below 5%. Fuel was stored in a tank and the pressures could be up to 16Mpa by a high pressure piston metering pump. Fuel flow rate was measured with a Coriolis-force flow meter (Model, DMF-1-1). A pressure gage transducer (Model 3051CA4, Rosemount) was used to measure the static pressure at the inlet of the test section, while a differential pressure transducer (Model, 3051CD4, Rosemount) was installed at both ends of the test section to measure the pressure drops. The fuel temperature was measured at inlet and exit with thermocouples. All data were recorded and logged onto the computer system.

Coolant Properties Composition analysis showed that RP-3 kerosene consists of 53% alkanes, 39% cycloalkanes, 5% benzenes and 3% naphthalenes¹. Accordingly, a 10-species surrogate was proposed, and the thermodynamic and transport properties as well as the critical point of this surrogate were then calculated with the NIST *Supertrapp*, a detailed discussion could be referred to [1]. **Fig. 2** is

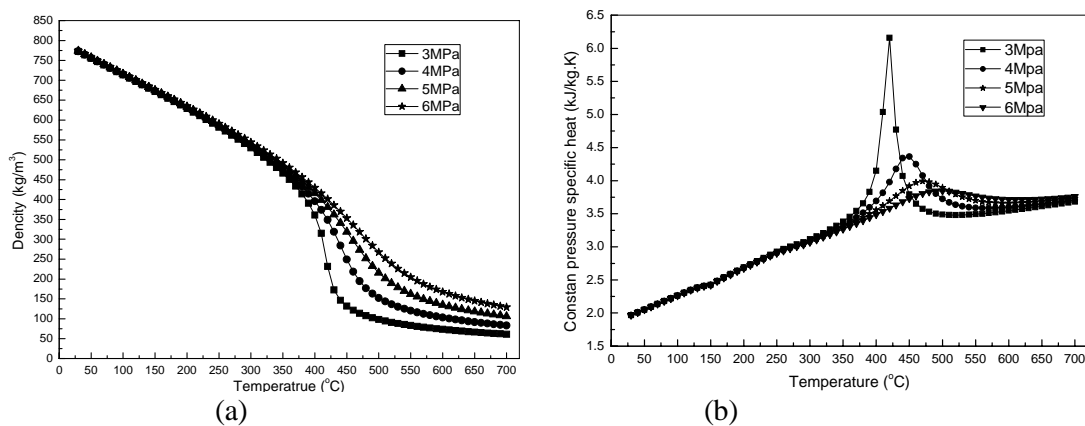


Fig. 2 Computed density and specific heat of the 10-species kerosene surrogate with temperature variation: (a) density and (b) specific heat

the calculated density and specific heat at constant pressure as a function of temperature. And the calculated critical temperature and critical pressure are respectively 387°C and 2.4MPa, while the measured critical temperature and pressure for RP-3 are respectively 372.35°C and 2.39MPa². Therefore, the calculated value of thermodynamic and transport properties are accurate and can be used to calculate other dimensionless numbers.

Procedure RP-3 pressure was maintained about 5MPa by the back pressure control valve and when RP-3 flow rate and pressure were stabilized, the electrical heating power supplies were turned on. The experimental data will then be recorded when the exit temperature reached near critical region. The local heat transfer coefficient h_x is defined by

$$h_x = \frac{q_x}{T_{wx,in} - T_{f,x}} \quad (1)$$

where the effective heat flux q_x is the difference of electrical energy and heat losses, the local fuel temperature $T_{f,x}$ was determined by the inlet and exit fuel temperature, and the inside wall temperature $T_{wx,in}$ was determined by solving the a 1D thermal conductivity equation under the cylindrical coordinate system as

$$\frac{k}{r} \frac{d}{dr} \left(r \frac{dT}{dr} \right) + \dot{\phi} = 0 \quad (2)$$

The boundary conditions were

$$q_{loss} = -k \left. \frac{dT}{dr} \right|_{r=r_{outo}} \quad (3)$$

and $T_{wx,out}$ was measured by thermocouple.

Then $T_{wx,in}$ is given by

$$T_{wx,in} = T_{wx,out} - \left[\left(\dot{\phi} \frac{r_{out}^2}{2} - q_{x,loss} r_{out} \right) \ln \frac{r_{out}}{r_{in}} - \frac{\dot{\phi}}{4} (r_{out}^2 - r_{in}^2) \right] / k_x \quad (4)$$

RESULTS AND ANALYSIS

Inlet Reynolds Number Fig. 3 is the local heat transfer coefficient h_x and the dimensionless inside wall temperature $T_{wx,in}/T_c$ variations along the tube with different inlet Reynolds numbers. BD is the bend diameter, and d and L are the tube inside diameter and the tube length respectively. Fig. 3

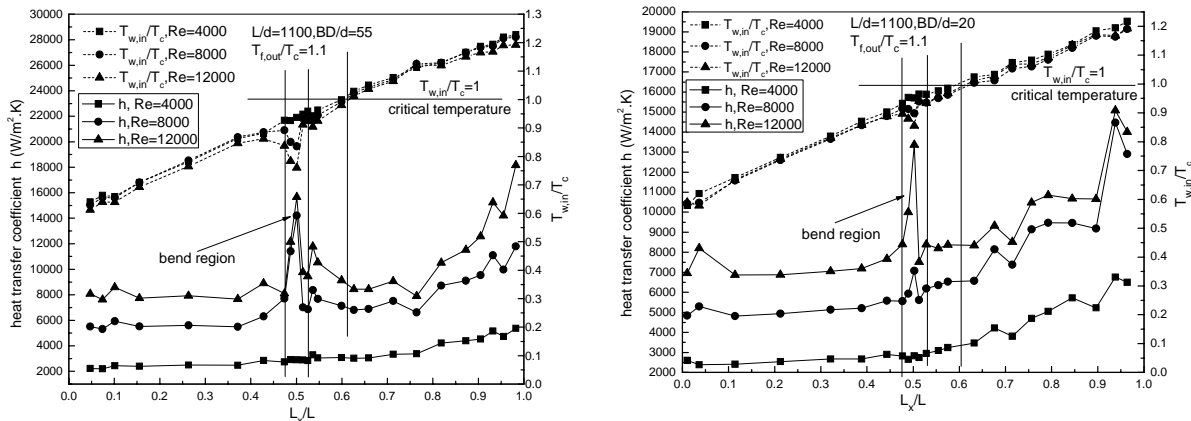


Figure 3. The influence of inlet Reynolds number on heat transfer

clearly indicated that the heat transfer coefficients were monotonously increasing along the tube for all experimental runs. Most of the passage 1(See Fig.1) showed a clear fully developed flow pattern and the heat transfer coefficients were nearly constant under the same inlet Reynolds number. In the bend regions, the heat transfer was enhanced due to the strong secondary flow induced by the centrifugal force and however, the enhancement was not obvious for low Reynolds number cases. The trans-critical process took place in the passage 2 and the exact location was dependent upon the inlet Reynolds number, the heating rate and other parameters. Heat transfer coefficient was enhanced due to

the phase change and the important physical properties such as density, specific heat, thermal conductivity, and dynamic viscosity etc., underwent a substantial change.

Bend Diameter Fig. 4 is the local heat transfer coefficient h_x and the dimensionless inside wall temperature $T_{wx,in}/T_c$ variations along tube with different dimensionless bend diameters (BD/d). It was within expectation that the increase of the bend diameter would increase the heat transfer coefficient due to the lengthening of the heavy secondary flow influencing passage and the shortening of the part where the flow was nearly fully developed and the thermal boundary layer was built-up. However, the exception was the case with BD/d=40 which had the lowest heat transfer coefficient as well as the dimensionless temperature. It should be mentioned that fluctuation was observed during the test for this case and the outlet temperature varied with time with a cycle about 8 to 14 seconds. The mechanism for the heat transfer coefficient drop as well as the fluctuation was unclear at the moment and it needs further investigation.

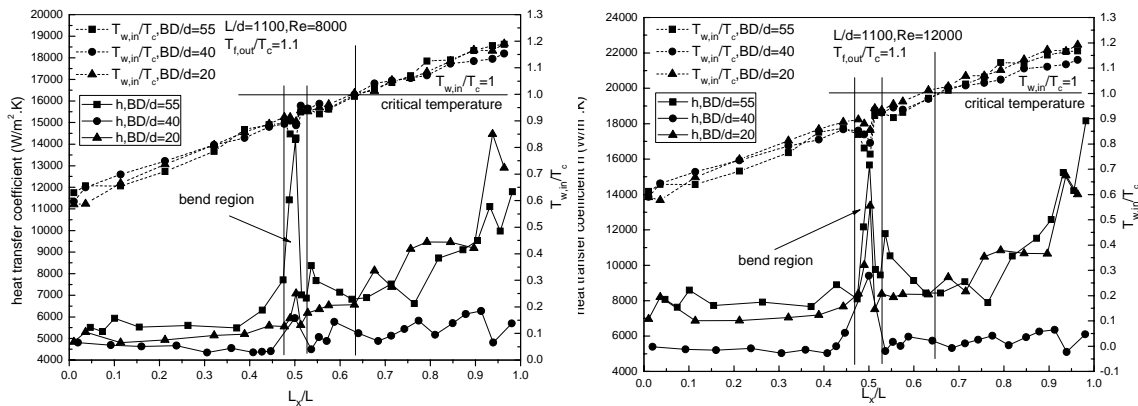


Figure 4. The influence of bend diameter on heat transfer

CONCLUSION

Test results indicated that the heat transfer coefficients were monotonously increasing along the tube for all experimental runs. In the bend regions, the heat transfer was enhanced due to the strong secondary flow induced by the centrifugal force and however, the enhancement was not obvious for low Reynolds number cases. And it was within expectation that the increase of the bend diameter would increase the heat transfer coefficient, however, the exception was the case with BD/d=40 which had the lowest heat transfer coefficient as well as the dimensionless temperature. The mechanism for the heat transfer coefficient drop was unclear at the moment and it needs further investigation.

REFERENCES

- Zhang, F-Q., Fan, X-J., Yu, G., Li, J-G., Liu, X-N. [2008], Heat Transfer of Aviation Kerosene at Supercritical Conditions, *AIAA-2008-4615*.
- Sun, Q-M. Mi, Z-T., Zhang, X-W. [2006], Determination of Critical Properties (ρ_c) of endothermic hydrocarbon fuels RP-3 and Simulated JP-7, *Journal of Fuel Chemistry and Technology, China, 0253-2409(2006)04-0466-05*.